

# Orbitally-Selective Breakdown of Fermi Liquid Quasiparticles in $\text{Ca}_{1.8}\text{Sr}_{0.2}\text{RuO}_4$

D. Sutter,<sup>1</sup> M. Kim,<sup>2,3</sup> C.E. Matt,<sup>1</sup> M. Horio,<sup>1</sup> R. Fittipaldi,<sup>4,5</sup> A. Vecchione,<sup>4,5</sup>  
V. Granata,<sup>4,5</sup> K. Hauser,<sup>1</sup> Y. Sassa,<sup>6</sup> G. Gatti,<sup>7</sup> M. Grioni,<sup>7</sup> M. Hoesch,<sup>8</sup> T. K. Kim,<sup>8</sup>  
E. Rienks,<sup>9</sup> N. C. Plumb,<sup>10</sup> M. Shi,<sup>10</sup> T. Neupert,<sup>1</sup> A. Georges,<sup>2,3,11,12</sup> and J. Chang<sup>1</sup>

<sup>1</sup>*Physik-Institut, Universität Zürich, Winterthurerstrasse 190, CH-8057 Zürich, Switzerland*

<sup>2</sup>*College de France, 75231 Paris Cedex 05, France*

<sup>3</sup>*Centre de Physique Théorique, Ecole Polytechnique,  
CNRS, Univ Paris-Saclay, 91128 Palaiseau, France*

<sup>4</sup>*CNR-SPIN, I-84084 Fisciano, Salerno, Italy*

<sup>5</sup>*Dipartimento di Fisica "E.R. Caianiello", Università di Salerno, I-84084 Fisciano, Salerno, Italy*

<sup>6</sup>*Department of Physics and Astronomy, Uppsala University, S-75121 Uppsala, Sweden*

<sup>7</sup>*Institute of Physics, École Polytechnique Fédérale de Lausanne (EPFL), CH-1015 Lausanne, Switzerland*

<sup>8</sup>*Diamond Light Source, Harwell Campus, Didcot, OX11 0DE, United Kingdom*

<sup>9</sup>*Helmholtz Zentrum Berlin, Bessy II, 12489 Berlin, Germany*

<sup>10</sup>*Swiss Light Source, Paul Scherrer Institut, CH-5232 Villigen PSI, Switzerland*

<sup>11</sup>*Department of Quantum Matter Physics, University of Geneva, 1211 Geneva 4, Switzerland*

<sup>12</sup>*Center for Computational Quantum Physics, Flatiron Institute, 162 5th av. New York NY 10010 USA*

We present a comprehensive angle-resolved photoemission spectroscopy study of  $\text{Ca}_{1.8}\text{Sr}_{0.2}\text{RuO}_4$ . Four distinct bands are revealed and along the Ru-O bond direction their orbital characters are identified through light polarisation analysis and comparison to dynamical mean field theory calculations. Bands assigned to  $d_{xz}$ ,  $d_{yz}$  orbitals display Fermi liquid behavior with four-fold quasi particle mass renormalization. Extremely heavy Fermions – associated with a predominantly  $d_{xy}$  band character – are shown to display non-Fermi liquid behavior. We thus demonstrate that  $\text{Ca}_{1.8}\text{Sr}_{0.2}\text{RuO}_4$  is a hybrid metal with an orbitally-selective Fermi liquid quasiparticle breakdown.

Correlated metals are typically classified either as Fermi liquids or non-Fermi liquids depending on whether resistivity scales with temperature squared or not. There is, however, transport evidence suggesting that some materials are hybrids of these two metal classes [1]. This mixed regime is of particular interest as it provides insight into how Fermi liquids break down and the nature of non-Fermi liquid quasiparticles. In this context, multi-orbital metallic systems in conjunction with strong Hund's coupling and electron correlations are of great conceptual importance [2]. Such Hund's metals are expected to display orbital differentiated quasiparticle (QP) renormalization effects along with magnetic correlations [3]. In the strongly correlated limit, orbitally selective Mott physics (OSMP) has been explored theoretically [4–9]. The concepts of Hund's metals and OSMP have both been applied to describe band structure renormalization effects in pnictide superconductor compounds [10–15]. It remains, however, unclear whether these systems exhibit genuine heavy Fermion and Mott physics. In contrast, the oxide compounds  $\text{LiV}_2\text{O}_4$  and  $\text{Ca}_{1.8}\text{Sr}_{0.2}\text{RuO}_4$  are multi-orbital systems where the existence of heavy Fermions are clearly demonstrated from specific heat measurements [16, 17].  $\text{Ca}_{1.8}\text{Sr}_{0.2}\text{RuO}_4$  is furthermore in close proximity to a Mott-Hubbard metal-insulator transition [18]. Angle resolved-photoemission experiments (ARPES) on this system have been interpreted in terms of both the Hund's metal and the OSMP scenario [19, 20]. Resistivity and specific heat indicate that the ground state is a Fermi liquid (FL). How-

ever, a thermal excitation of just 1 K turns the system into a non-Fermi liquid (nFL) state [16]. Here we present a high-resolution ARPES study, demonstrating that  $\text{Ca}_{1.8}\text{Sr}_{0.2}\text{RuO}_4$  is neither a standard Hunds metal nor representing OSMP. In fact, the thermally excited state constitutes an example of a hybrid metal. Along the Ru-O bond direction, bands with  $d_{xz}$ ,  $d_{yz}$  orbital character display FL behavior whereas  $d_{xy}$  dominated bands host nFL QPs. Breakdown of FL QPs are therefore orbitally selective. This physics might apply to other ruthenate systems such as for example  $\text{Sr}_3\text{Ru}_2\text{O}_7$ .

Single crystals of  $\text{Ca}_{1.8}\text{Sr}_{0.2}\text{RuO}_4$  were grown by the flux-feeding floating-zone technique [30, 31]. ARPES experiments were carried out at I05, SIS, 1<sup>3</sup> beamlines of Diamond Light Source (DLS) [32], Swiss Light Source (SLS), and BESSY – respectively. All samples were cleaved *in-situ* under UHV conditions and measured at temperatures  $T = 1 - 30$  K. ARPES spectra were collected with different incident photon energies  $h\nu$  and light polarisations using Scienta R4000 electron analyzers. Depending on  $h\nu$  and  $T$ , the overall energy resolution was in the order of 10 meV. As  $\text{Ca}_{1.8}\text{Sr}_{0.2}\text{RuO}_4$  has low-temperature L-Pbca [33] crystal structure ( $a = 5.33$  Å,  $b = 5.32$  Å and  $c = 12.41$  Å), orthorhombic notation is used. The electronic structure is calculated within the DFT+DMFT (density functional theory + dynamical mean field theory) framework using Wien2k [34] and the TRIQS library [35–37], including a strong-coupling continuous-time Monte Carlo impurity solver [38, 39].

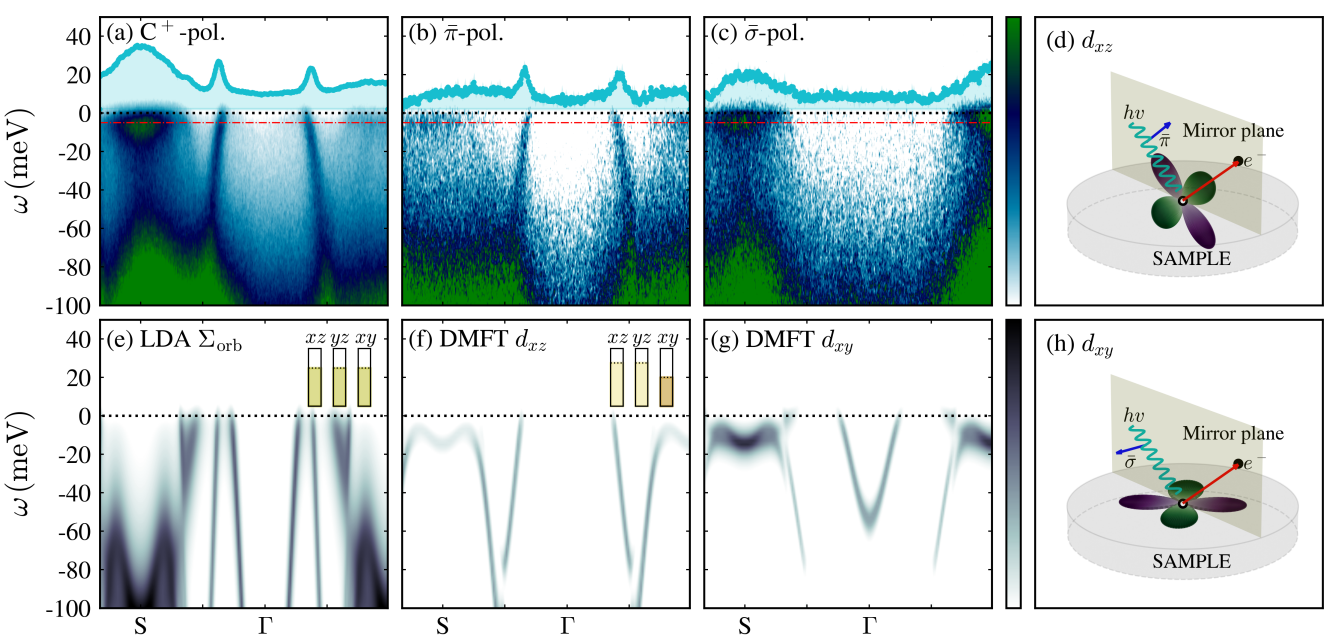
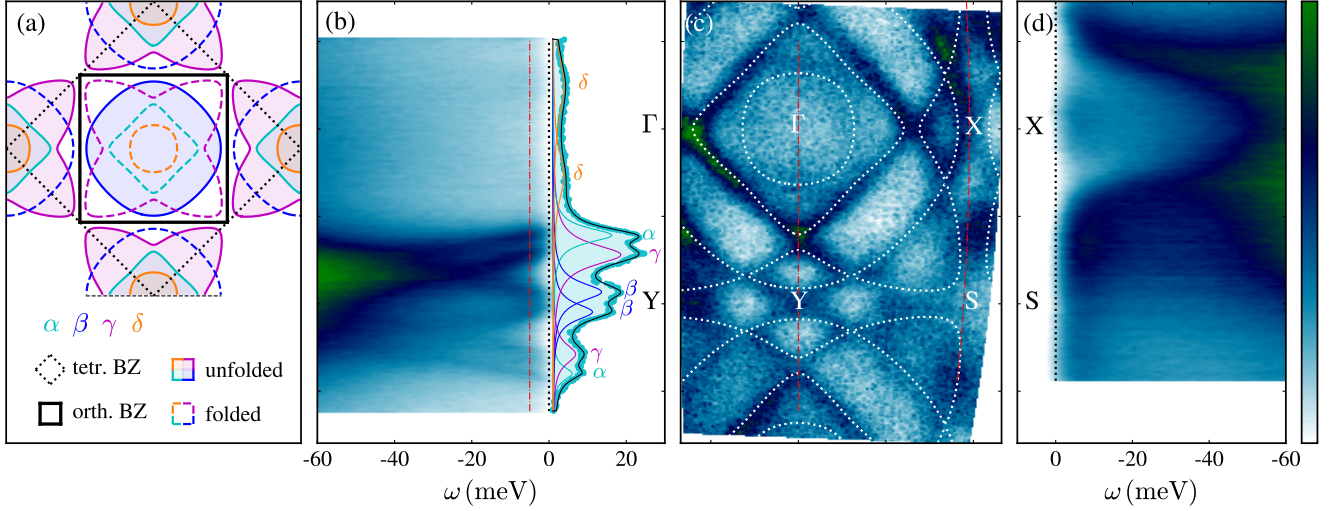


FIG. 2. Heavy fermion QPs and orbital band character. (a–c) ARPES spectra along the zone diagonal ( $\Gamma$ -S) using 40 eV circularly-,  $\bar{\sigma}$ -, and  $\bar{\pi}$ -polarisation, respectively. Cyan points are MDCs near  $E_F$  (dashed turquoise lines). (d, h) Schematics for photoemission selection rules for  $d_{xy}$  and  $d_{xz}$  orbitals. (e) DFT band structure along  $\Gamma$ -S. (f, g) DMFT calculation of the spectral function orbitally resolved. To mimic the experimental data, the DFT and DMFT calculations are plotted in spectral representation, truncated by the Fermi-Dirac distribution ( $T_{\text{DMFT}} = 39$  K), and a constant inverse lifetime of 20 meV is used. Relative orbital fillings are indicated by the insets in (e, f).

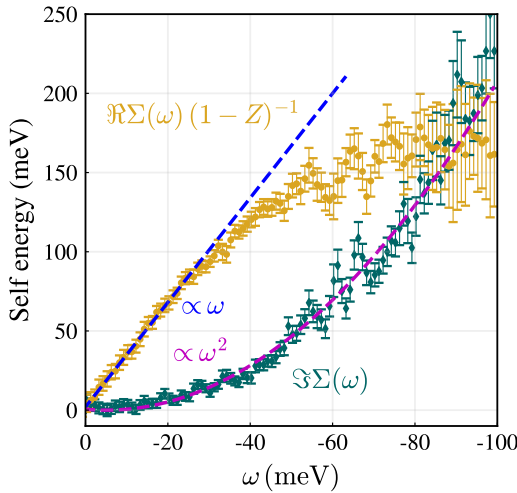


FIG. 3. Self-energy  $\Sigma(\omega)$  of the  $\alpha$ -band, plotted as  $\Im\Sigma(\omega)$  (green points) and  $\Re\Sigma(\omega)/(1-Z)$  (yellow points) versus binding energy  $\omega$ . Dashed lines are fits to quadratic and linear dependencies, respectively. For  $\Re\Sigma(\omega)/(1-Z)$ , the fit is restricted to the low- $\omega$  regime.

Wannier-like  $t_{2g}$  orbitals are constructed out of Kohn-Sham bands within the energy window  $[-2, 1]$  eV with respect to the Fermi energy  $E_F$ . For the correct description of atomic multiplets, a rotationally invariant Kanamori interaction is used [2]. Inclusion of charge-self-consistency in the DFT+DMFT loop does not change our results. This validates the correlation induced changes of orbital occupancy in the DFT+DMFT in comparison with the DFT result.

Bulk  $\text{Sr}_2\text{RuO}_4$  hosts three Fermi surface (FS) sheets  $\alpha$ ,  $\beta$  ( $d_{xz}$ ,  $d_{yz}$ ) and  $\gamma$  ( $d_{xy}$ ) [22, 40–46]. Upon Ca for Sr substitution, the  $\gamma$ -band is undergoing a Lifshitz transition, changing it from electron- to hole-like [29]. Simultaneously, an electron pocket emerging around the zone center is predicted [47]. Orthorhombic folding of these bands (shown schematically in Fig. 1a) captures all the observed FS sheets of  $\text{Ca}_{1.8}\text{Sr}_{0.2}\text{RuO}_4$ . In total four sheets are observed and labelled  $\alpha$ ,  $\beta$ ,  $\gamma$  and  $\delta$  (Fig. 1b–d). The weakest  $\delta$ -band is further documented in the Supplementary Material (SM) SFig. 1 [21] and light polarisation dependence of the  $\alpha$  and  $\gamma$  bands is shown in Fig. 2. The  $\alpha$ -band, observed with  $C^+$  and  $\bar{\pi}$ -polarised light, is suppressed completely in the  $\bar{\sigma}$ -channel. For the  $\gamma$ -band in the zone corner, the opposite trend is observed although complete suppression is not found. Self-energy  $\Sigma(\omega)$  versus temperature and binding energy  $\omega$  is extracted through a combination of momentum and energy distribution curve (EDC) analysis. For example, the  $\alpha$ -band QP dispersion is analyzed by fitting momentum distribution curves (MDC). The resulting band dispersion  $\varepsilon_k^\alpha$  and line-width  $\Gamma(\omega)$  led us to  $\Re\Sigma(\omega) = \varepsilon_k^\alpha - \varepsilon_k^b$  and

$\Im\Sigma(\omega) = \Gamma(\omega)v_F^b$  where  $\varepsilon_k^b$  and  $v_F^b$  are the DFT bare band and associated Fermi velocity (Fig. 3). Temperature dependence of spectral intensity along the zone diagonal for both the  $\alpha$ - and  $\gamma$ -band are analyzed in Fig. 4. In contrast to the  $\alpha$ -sheet, the  $\gamma$ -band QP peak amplitude has significant  $T$ -dependence.

DFT calculations provide an excellent description of the experimental FS of  $\text{Sr}_2\text{RuO}_4$  [43]. Already without spin-orbit coupling (SOC), our DFT calculation of  $\text{Ca}_{1.8}\text{Sr}_{0.2}\text{RuO}_4$  produces several of the experimentally observed FS sheets (Fig. 2e). SOC is known to improve the calculation along the  $\Gamma$ -Y direction [43, 48], but has no effect along the  $\Gamma$ -S direction. The absence of the heavy Fermi pocket around the S-point in the DFT calculation is therefore a significant discrepancy (compare Fig. 2a, e). This motivated our DMFT calculations, using the same parameters of Coulomb interaction  $U = 2.3$  eV and Hund's coupling  $J_H = 0.4$  eV that successfully described  $\text{Ca}_2\text{RuO}_4$  [49] and other ruthenates [3, 50]. DMFT predicts strong bandwidth renormalization effects, which is particularly clear for the  $\delta$ -band (see Fig. 2g). Moreover, our DMFT calculation reproduces qualitatively the heavy Fermions states around the zone corner.

Next, we discuss the orbital character of the  $\alpha$  and  $\gamma$  bands along  $\Gamma$ -S. The incident light and centre of our analyser slit, define a mirror plane to which the electromagnetic field has odd (even) parity for  $\bar{\sigma}$  ( $\bar{\pi}$ ) polarisation (see Fig. 2d,h). For final states with even character, selection rules [51] dictate that odd (even) band character is suppressed in the  $\bar{\pi}$  ( $\bar{\sigma}$ ) polarisation channel. The  $\alpha$ -band being suppressed completely (see Fig. 2) in the  $\bar{\sigma}$ -channel therefore has even character. Assuming approximately tetragonal crystal structure, ( $d_{xy}$ ,  $d_{xz}$ , and  $d_{yz}$ ) have (odd, even, and odd) character along the  $a$ -axis. As a result and consistent with the DFT and DMFT calculations, the  $\alpha$ -band along the Ru-O bond direction has pure  $d_{xz}$  character. The  $\gamma$ -band is placed further away from the mirror-plane due to the perpendicular electron analyser-slit. Hence, less strict selection rules are expected. Nevertheless, our experimental results and DMFT calculations both assign predominately  $d_{xy}$  character to the  $\gamma$ -band.

As Hund's coupling quenches inter-orbital fluctuations, the orbitals can be viewed approximately as single bands [2, 52, 53]. For the ruthenates, this is valid only along the  $\Gamma$ -S direction as spin-orbit interaction mixes orbital characters along  $\Gamma$ -Y [43]. Experimentally, it is thus only sensible to evaluate orbital differentiated properties along  $\Gamma$ -S. Comparison of DFT and DMFT suggests that the  $d_{xy}$  dominated  $\delta$ - and  $\gamma$ -bands are most strongly affected by electron correlations. It suggests that electron correlations are orbitally differentiated. Orbital fillings provide some insight into this effect. As the  $\text{RuO}_4$  octahedron is almost cubic, DFT yields essentially degenerate  $d_{xy}$ ,  $d_{xz}$ , and  $d_{yz}$  orbital energies with equivalent 4/3-

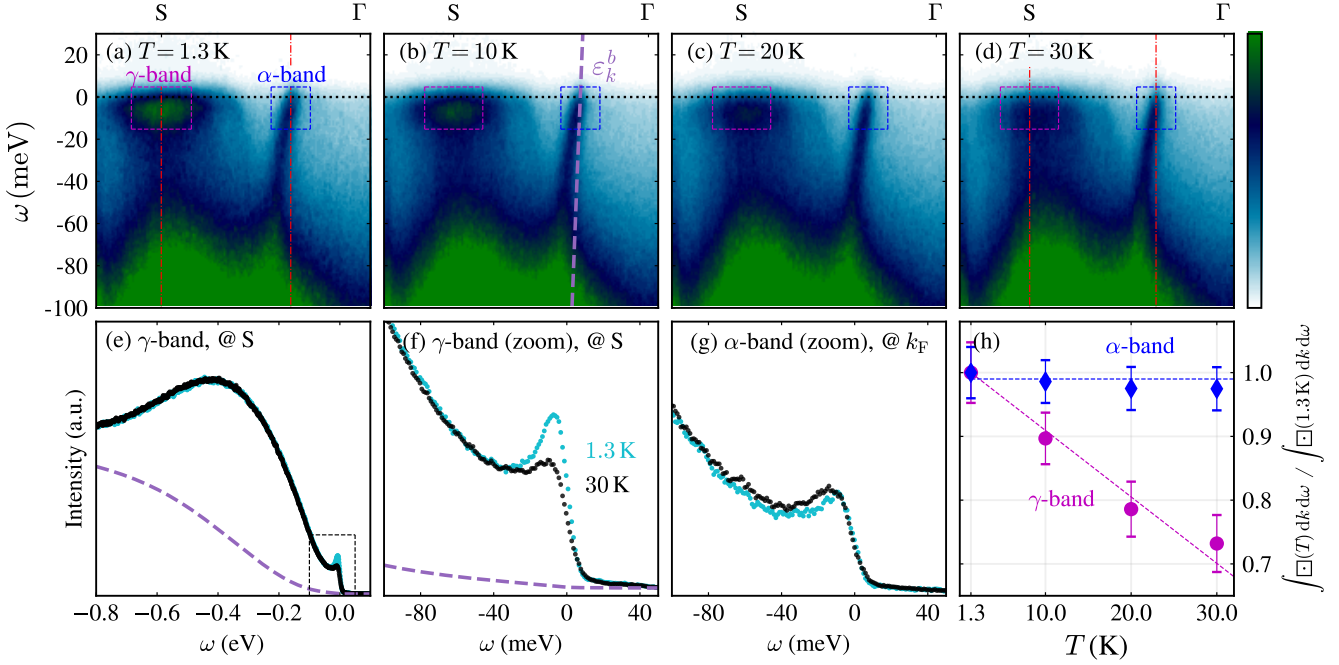


FIG. 4. Temperature dependence of QP spectral weight. (a–d) ARPES spectra along S–Γ for temperatures as indicated with DFT bare band dispersion  $\varepsilon_k^b$  in (b). (e–g) Raw data EDCs of the  $\alpha$ - and  $\gamma$ -band at  $T = 1.3$  K (cyan) and  $30$  K (black) and fixed momenta indicated by dashed vertical lines in (a) and (d). (f) is a zoom near  $E_F$  of the EDC displayed in (e). Dashed lines in (e,f) indicate a Shirley background. (h) Normalized spectral weight, integrated within the magenta ( $\gamma$ ) and blue ( $\alpha$ ) boxes shown in (a–d), versus  $T$ .

filling (inset Fig. 2e). The DMFT calculations, by contrast, indicate that electron interactions favor a less populated  $d_{xy}$  orbital with  $(n_{xy}, n_{xz}, n_{yz}) = (1.18, 1.42, 1.42)$  (inset Fig. 2f). Electron interactions thus push the  $d_{xy}$  channel closer to half-filling and effectively into a more correlated regime.

To describe the orbitally differentiated self-energy of  $\text{Ca}_{1.8}\text{Sr}_{0.2}\text{RuO}_4$ , we distinguish between saturated and unsaturated FLs. The latter refers to QPs for which  $Z$  has  $\omega$  or temperature dependence. This implies a nFL self-energy, *i.e.*, non-linear  $\Re\Sigma(\omega)$  for  $\omega \rightarrow 0$ . The saturated regime, by contrast, refers to a standard FL with self-energy  $\Sigma(\omega, T) = \gamma_0\omega + i\alpha_0[\omega^2 + (\pi k_B T)^2]$  where  $\gamma_0$  and  $\alpha_0$  are constants [51, 54]. Hence, the QP residue  $Z \equiv [1 - \partial_\omega \Re\Sigma(\omega)]^{-1} = (1 - \gamma_0)^{-1}$  is independent of  $\omega$  and  $T$ . A FL is therefore expected to display (1) a linear QP dispersion, (2) a line width that scales as  $\omega^2$ ,  $Z|\Im\Sigma(\omega)| < \omega$  [55] below a cut-off energy scale, and (4) a QP amplitude proportional to  $Z$ , independent of  $\omega$  and  $T$ . Using  $\Re\Sigma(\omega) = \omega(1 - 1/Z)$ , the third criterion can be rewritten as  $|\Im\Sigma(\omega)| < \Re\Sigma(\omega)/(1 - Z)$ . For criterion four, the Fermi-Dirac distribution combined with finite instrumental resolution may induce a weak temperature dependence on the effectively observed QP peak amplitude. This weak effect is discussed in the SM Note I [21]. Examination of the  $\alpha$

band, with pure  $d_{xz}$ ,  $d_{yz}$  character, reveals an almost  $T$ -independent QP amplitude (Fig. 4g). The QP dispersion is approximately linear  $\varepsilon_k^\alpha \approx v_F|k - k_F|$ , implying  $\Re\Sigma(\omega) = (1 - v_F^b/v_F)\omega$ , with  $v_F$  and  $v_F^b$  being dressed and bare Fermi velocities [56]. Assuming an isotropic FL and using  $v_F^b = 2.34 \text{ eV}\text{\AA}$ , the QP residue yields  $Z = v_F/v_F^b = 0.26(4)$ , consistent with DMFT that finds  $Z_{xz} = 0.23$ . Analysis of the MDC linewidth (HWHM) at  $T = 30$  K yields  $\Gamma(\omega) = \Gamma_0 + \eta\omega^2$  with  $\Gamma_0 = 0.020(2) \text{ \AA}^{-1}$  and  $\eta = 10.6(6) \text{ \AA}^{-1}\text{eV}^{-2}$  being constants. This is documented by plotting  $\Im\Sigma(\omega) = (\Gamma(\omega) - \Gamma_0)v_F^b$  versus  $\omega$  (Fig. 3). By comparing  $\Re\Sigma(\omega)/(1 - Z)$  and  $\Im\Sigma(\omega)$ , criterion three is obviously satisfied and as shown in Fig. 4g,h the quasiparticle amplitude is temperature independent. The QP excitations of the  $\alpha$ -band thus fulfil, in the most strict sense, all criteria of a FL (see also SM SFig. 5 [21]).

Resistivity and specific heat measurements, however, display FL behavior for  $T < 1$  K only and much heavier QP masses [16]. Reconciliation is reached by analysis of the extremely dressed  $\gamma$ -band QP states around the S-point. These QP amplitudes are roughly proportional to  $Z$ . In contrast to the  $\alpha$ -band, the QP peak amplitude of the  $\gamma$ -band exhibits a pronounced suppression with increased  $T$  (Fig. 4e–g). To circumvent the effects of (i) the Fermi-Dirac distribution, (ii) impurity scattering and (iii) finite instrumental resolution (see SM SFig. 3

and 4 [21]), it is useful to perform a box integration of spectral weight around  $k_F$  (see Fig. 4a–d). Again, the  $\gamma$ -band displays a pronounce spectral weight temperature dependence whereas the  $\alpha$ -band remains approximately unchanged. As both the  $\alpha$ - and  $\gamma$ -bands are measured simultaneously, this effect is not a result of surface degradation. We are thus led to conclude that the  $d_{xy}$  dominated  $\gamma$ -band states display non-saturated FL behavior. Furthermore, the ratio between coherent and incoherent spectral weight (see Fig. 4e) indicates that  $Z \ll 1$  around the S-point, in accordance with the DMFT value  $Z_{xy} \approx 0.05$ . We have thus demonstrated that the QP mass renormalization and FL QP breakdown are orbitally selective along the  $\Gamma$ -S direction. It is also worth noticing that temperature dependent spectral weight has also been reported in CeCoIn<sub>5</sub> [57] and Ce<sub>2</sub>PdIn<sub>8</sub> [58]. This effect may therefore be generic to heavy fermion quasiparticles.

In summary, we have presented a combined ARPES, DFT, and DMFT study of Ca<sub>1.8</sub>Sr<sub>0.2</sub>RuO<sub>4</sub>. Our results revealed the complete low-energy electronic structure. Through light polarisation analysis and band structure calculations, insight into the orbital band character was obtained. By studying self-energy effects, it was demonstrated that QP masses and the FL breakdown are orbitally selective. Ca<sub>1.8</sub>Sr<sub>0.2</sub>RuO<sub>4</sub> thus constitutes a unique example of a hybrid metal hosting orbitally differentiated FL and nFL QPs. As an outlook, it is interesting to consider the idea that nFL behavior found in Ba<sub>2</sub>RuO<sub>4</sub> [59] and Sr<sub>2</sub>RuO<sub>4</sub> [60] under strain has a similar underlying origin.

D.S., M.H., T.N., and J.C. acknowledge support by the Swiss National Science Foundation and Y.S. was supported by the Wenner-Gren foundation. Experiments were carried out on the I05, SIS, and 1<sup>3</sup> endstations at the Diamond Light Source, Swiss Light Source and BESSY, respectively. We acknowledge Diamond Light Source for time on beamline I05 under proposal SI15296. A.G. and M.K. acknowledge the support of the European Research Council grant ERC-319286-QMAC and the Swiss National Science Foundation (NCCR MARVEL), as well as support from the CPHT computer team. The Flatiron Institute is supported by the Simons Foundation. We thank all beamline staff for technical support.

- 
- [1] R. A. Cooper, Y. Wang, B. Vignolle, O. J. Lipscombe, S. M. Hayden, Y. Tanabe, T. Adachi, Y. Koike, M. Nozawa, H. Takagi, C. Proust, and N. E. Hussey, *Science* **323**, 603 (2009).
- [2] A. Georges, L. de' Medici, and J. Mravlje, *Annu. Rev. Condens. Matter Phys.* **4**, 137 (2013).
- [3] J. Mravlje, M. Aichhorn, T. Miyake, K. Haule, G. Kotliar, and A. Georges, *Phys. Rev. Lett.* **106**, 096401 (2011).
- [4] V. I. Anisimov, I. A. Nekrasov, D. E. Kondakov, T. Rice, and M. Sigrist, *Eur. Phys. J. B* **25**, 191 (2002).
- [5] A. Koga, N. Kawakami, T. M. Rice, and M. Sigrist, *Phys. Rev. Lett.* **92**, 216402 (2004).
- [6] M. Vojta, *J. Low Temp. Phys.* **161**, 203 (2010).
- [7] L. de'Medici, A. Georges, and S. Biermann, *Phys. Rev. B* **72**, 205124 (2005).
- [8] S. Biermann, L. de' Medici, and A. Georges, *Phys. Rev. Lett.* **95**, 206401 (2005).
- [9] M. Ferrero, F. Becca, M. Fabrizio, and M. Capone, *Phys. Rev. B* **72**, 205126 (2005).
- [10] Z. P. Yin, K. Haule, and G. Kotliar, *Nat. Phys.* **7**, 294 (2011).
- [11] M. Yi, Z.-K. Liu, Y. Zhang, R. Yu, J. X. Zhu, J. J. Lee, R. G. Moore, F. T. Schmitt, W. Li, S. C. Riggs, J. H. Chu, B. Lv, J. Hu, M. Hashimoto, S. K. Mo, Z. Hussain, Z. Q. Mao, C. W. Chu, I. R. Fisher, Q. Si, Z. X. Shen, and D. H. Lu, *Nat Commun.* **6**, 7777 (2015).
- [12] S. Gerber, S.-L. Yang, D. Zhu, H. Soifer, J. A. Sobota, S. Rebec, J. J. Lee, T. Jia, B. Moritz, C. Jia, A. Gauthier, Y. Li, D. Leuenberger, Y. Zhang, L. Chaix, W. Li, H. Jang, J.-S. Lee, M. Yi, G. L. Dakovski, S. Song, J. M. Glownia, S. Nelson, K. W. Kim, Y.-D. Chuang, Z. Hussain, R. G. Moore, T. P. Devereaux, W.-S. Lee, P. S. Kirchmann, and Z.-X. Shen, *Science* **357**, 71 (2017).
- [13] P. O. Sprau, A. Kostin, A. Kreisel, A. E. Böhmer, V. Taufour, P. C. Canfield, S. Mukherjee, P. J. Hirschfeld, B. M. Andersen, and J. C. S. Davis, *Science* **357**, 75 (2017).
- [14] M. Aichhorn, S. Biermann, T. Miyake, A. Georges, and M. Imada, *Phys. Rev. B* **82**, 064504 (2010).
- [15] D.-H. Lee, *Science* **357**, 32 (2017).
- [16] S. Nakatsuji, D. Hall, L. Balicas, Z. Fisk, K. Sugahara, M. Yoshioka, and Y. Maeno, *Phys. Rev. Lett.* **90**, 137202 (2003).
- [17] S. Kondo, D. C. Johnston, C. A. Swenson, F. Borsa, A. V. Mahajan, L. L. Miller, T. Gu, A. I. Goldman, M. B. Maple, D. A. Gajewski, E. J. Freeman, N. R. Dilley, R. P. Dickey, J. Merrin, K. Kojima, G. M. Luke, Y. J. Uemura, O. Chmaisssem, and J. D. Jorgensen, *Phys. Rev. Lett.* **78**, 3729 (1997).
- [18] S. Nakatsuji, V. Dobrosavljević, D. Tanasković, M. Minakata, H. Fukazawa, and Y. Maeno, *Phys. Rev. Lett.* **93**, 146401 (2004).
- [19] A. Shimoyamada, K. Ishizaka, S. Tsuda, S. Nakatsuji, Y. Maeno, and S. Shin, *Phys. Rev. Lett.* **102**, 086401 (2009).
- [20] M. Neupane, P. Richard, Z.-H. Pan, Y.-M. Xu, R. Jin, D. Mandrus, X. Dai, Z. Fang, Z. Wang, and H. Ding, *Phys. Rev. Lett.* **103**, 097001 (2009).
- [21] A. r. e. t. b. m. See Supplementary Material for details concerning  $\delta$ -band identification, Self-energy DMFT calculations and the band structure fitting procedure., .
- [22] V. B. Zabolotnyy, D. V. Evtushinsky, A. A. Kordyuk, T. K. Kim, E. Carleschi, B. P. Doyle, R. Fittipaldi, M. Cuoco, A. Vecchione, and S. V. Borisenko, *Journal of Electron Spectroscopy and Related Phenomena* **191**, 48 (2013).
- [23] W.-C. Lee, D. P. Arovas, and C. Wu, *Phys. Rev. B* **81**, 184403 (2010).
- [24] C. M. Puett, J. G. Rau, and H.-Y. Kee, *Phys. Rev. B* **81**, 081105 (2010).
- [25] K. K. Ng and M. Sigrist, *EPL* **49**, 473 (2000).

- [26] C. G. Fatuzzo, M. Dantz, S. Fatale, P. Olalde-Velasco, N. E. Shaik, B. Dalla Piazza, S. Toth, J. Pelliciari, R. Fittipaldi, A. Vecchione, N. Kikugawa, J. S. Brooks, H. M. Rønnow, M. Grioni, C. Rüegg, T. Schmitt, and J. Chang, *Phys. Rev. B* **91**, 155104 (2015).
- [27] T. Mizokawa, L. H. Tjeng, G. A. Sawatzky, G. Ghiringhelli, O. Tjernberg, N. B. Brookes, H. Fukazawa, S. Nakatsuji, and Y. Maeno, *Phys. Rev. Lett.* **87**, 077202 (2001).
- [28] D. Kingma P. and J. Ba, [arXiv:1412.6980](#) (2014).
- [29] S.-C. Wang, H.-B. Yang, A. K. P. Sekharan, S. Souma, H. Matsui, T. Sato, T. Takahashi, C. Lu, J. Zhang, R. Jin, D. Mandrus, E. W. Plummer, Z. Wang, and H. Ding, *Phys. Rev. Lett.* **93**, 177007 (2004).
- [30] H. Fukazawa, S. Nakatsuji, and Y. Maeno, *Physica B Condens Matter* **281**, 613 (2000).
- [31] S. Nakatsuji and Y. Maeno, *J Solid State Chem* **156**, 26 (2001).
- [32] M. Hoesch, T. K. Kim, P. Dudin, H. Wang, S. Scott, P. Harris, S. Patel, M. Matthews, D. Hawkins, S. G. Alcock, T. Richter, J. J. Mudd, M. Basham, L. Pratt, P. Leicester, E. C. Longhi, A. Tamai, and F. Baumberger, *Review of Scientific Instruments* **88**, 013106 (2017).
- [33] O. Friedt, M. Braden, G. André, P. Adelmann, S. Nakatsuji, and Y. Maeno, *Phys. Rev. B* **63**, 174432 (2001).
- [34] P. Blaha, K. Schwarz, G. Madsen, D. Kvasnicka, and J. Luitz, *TU Wien* (2001).
- [35] M. Aichhorn, L. Pourovskii, V. Vildosola, M. Ferrero, O. Parcollet, T. Miyake, A. Georges, and S. Biermann, *Phys. Rev. B* **80**, 085101 (2009).
- [36] M. Aichhorn, L. Pourovskii, P. Seth, V. Vildosola, M. Zingl, O. E. Peil, X. Deng, J. Mravlje, G. J. Kraberger, C. Martins, M. Ferrero, and O. Parcollet, *Computer Physics Communications* **204**, 200 (2016).
- [37] O. Parcollet, M. Ferrero, T. Ayral, H. Hafermann, I. Krivenko, L. Messio, and P. Seth, *Computer Physics Communications* **196**, 398 (2015).
- [38] E. Gull, A. J. Millis, A. I. Lichtenstein, A. N. Rubtsov, M. Troyer, and P. Werner, *Rev. Mod. Phys.* **83**, 349 (2011).
- [39] P. Seth, I. Krivenko, M. Ferrero, and O. Parcollet, *Comput. Phys. Commun.* **200**, 274 (2016).
- [40] A. Damascelli, D. H. Lu, K. M. Shen, N. P. Armitage, F. Ronning, D. L. Feng, C. Kim, Z.-X. Shen, T. Kimura, Y. Tokura, Z. Q. Mao, and Y. Maeno, *Phys. Rev. Lett.* **85**, 5194 (2000).
- [41] C. Bergemann, A. P. Mackenzie, S. R. Julian, D. Forsythe, and E. Ohmichi, *Advances in Physics* **52**, 639 (2003).
- [42] V. B. Zabolotnyy, E. Carleschi, T. K. Kim, A. A. Korodyuk, J. Trinckauf, J. Geck, D. Evtushinsky, B. P. Doyle, R. Fittipaldi, M. Cuoco, A. Vecchione, B. Bchner, and S. V. Borisenko, *New Journal of Physics* **14**, 063039 (2012).
- [43] M. W. Haverkort, I. S. Elfimov, L. H. Tjeng, G. A. Sawatzky, and A. Damascelli, *Phys. Rev. Lett.* **101**, 026406 (2008).
- [44] H. Iwasawa, Y. Yoshida, I. Hase, S. Koikegami, H. Hayashi, J. Jiang, K. Shimada, H. Namatame, M. Taniguchi, and Y. Aiura, *Phys. Rev. Lett.* **105**, 226406 (2010).
- [45] H. Iwasawa, Y. Yoshida, I. Hase, K. Shimada, H. Namatame, M. Taniguchi, and Y. Aiura, *Phys. Rev. Lett.* **109**, 066404 (2012).
- [46] T. Kondo, M. Ochi, M. Nakayama, H. Taniguchi, S. Akebi, K. Kuroda, M. Arita, S. Sakai, H. Namatame, M. Taniguchi, Y. Maeno, R. Arita, and S. Shin, *Phys. Rev. Lett.* **117**, 247001 (2016).
- [47] E. Ko, B. J. Kim, C. Kim, and H. J. Choi, *Phys. Rev. Lett.* **98**, 226401 (2007).
- [48] M. Kim, J. Mravlje, M. Ferrero, O. Parcollet, and A. Georges, *Phys. Rev. Lett.* **120**, 126401 (2018).
- [49] D. Sutter, C. G. Fatuzzo, S. Moser, M. Kim, R. Fittipaldi, A. Vecchione, V. Granata, Y. Sassa, F. Cossalter, G. Gatti, M. Grioni, H. M. Rønnow, N. C. Plumb, C. E. Matt, M. Shi, M. Hoesch, T. K. Kim, T.-R. Chang, H.-T. Jeng, C. Jozwiak, A. Bostwick, E. Rotenberg, A. Georges, T. Neupert, and J. Chang, *Nature Communications* **8**, 15176 (2017).
- [50] H. T. Dang, J. Mravlje, A. Georges, and A. J. Millis, *Phys. Rev. B* **91**, 195149 (2015).
- [51] A. Damascelli, Z. Hussain, and Z.-X. Shen, *Rev. Mod. Phys.* **75**, 473 (2003).
- [52] L. de' Medici, G. Giovannetti, and M. Capone, *Phys. Rev. Lett.* **112**, 177001 (2014).
- [53] L. de' Medici, J. Mravlje, and A. Georges, *Phys. Rev. Lett.* **107**, 256401 (2011).
- [54] C. M. Varma, Z. Nussinov, and W. van Saarloos, *Phys. Rep.* **361**, 267 (2002).
- [55] X. Deng, J. Mravlje, R. Žitko, M. Ferrero, G. Kotliar, and A. Georges, *Phys. Rev. Lett.* **110**, 086401 (2013).
- [56] C. G. Fatuzzo, Y. Sassa, M. Måansson, S. Pailhès, O. J. Lipscombe, S. M. Hayden, L. Patthey, M. Shi, M. Grioni, H. M. Rønnow, J. Mesot, O. Tjernberg, and J. Chang, *Phys. Rev. B* **89**, 205104 (2014).
- [57] Q. Y. Chen, D. F. Xu, X. H. Niu, J. Jiang, R. Peng, H. C. Xu, C. H. P. Wen, Z. F. Ding, K. Huang, L. Shu, Y. J. Zhang, H. Lee, V. N. Strocov, M. Shi, F. Bisti, T. Schmitt, Y. B. Huang, P. Dudin, X. C. Lai, S. Kirchner, H. Q. Yuan, and D. L. Feng, *Phys. Rev. B* **96**, 045107 (2017).
- [58] Q. Yao, D. Kaczorowski, P. Swatek, D. Gnida, C. H. P. Wen, X. H. Niu, R. Peng, H. C. Xu, P. Dudin, S. Kirchner, Q. Y. Chen, D. W. Shen, and D. L. Feng, *Phys. Rev. B* **99**, 081107 (2019).
- [59] B. Burganov, C. Adamo, A. Mulder, M. Uchida, P. D. C. King, J. W. Harter, D. E. Shai, A. S. Gibbs, A. P. Mackenzie, R. Uecker, M. Bruetzam, M. R. Beasley, C. J. Fennie, D. G. Schlom, and K. M. Shen, *Phys. Rev. Lett.* **116**, 197003 (2016).
- [60] M. E. Barber, A. S. Gibbs, Y. Maeno, A. P. Mackenzie, and C. W. Hicks, *Phys. Rev. Lett.* **120**, 076602 (2018).